Journal of information and communication convergence engineering
http://jicce.org

J. Inf. Commun. Converg. Eng. 21(3): 233-238, Sep. 2023 **Regular paper**

Identification of Partial Discharge Defects based on Back-Propagation Algorithm in Eco-friendly Insulation Gas

Sung-Wook Kim*, ***Member, KIICE***

Department of Electrical and Electronics Engineering, Silla University, 46958, Korea

Abstract

This study presents a method for identifying partial discharge defects in an eco-friendly gas insulated system using a back-propagation algorithm. Four partial discharge (PD) electrode systems, namely, a free-moving particle, protrusion on the conductor, protrusion on the enclosure, and voids, were designed to simulate PD defects that can occur during the operation of eco-friendly gas-insulated switchgear. The PD signals were measured using an ultrahigh-frequency sensor as a nonconventional method based on IEC 62478. To identify the types of PD defects, the PD parameters of single PD pulses in the time and frequency domains and the phase-resolved partial discharge patterns were extracted, and a back-propagation algorithm in the artificial neural network was designed using a virtual instrument based on LabVIEW. The backpropagation algorithm proposed in this paper has an accuracy rate of over 90% for identifying the types of PD defects, and the result is expected to be used as a reference database for asset management and maintenance work for eco-friendly gas-insulated power equipment.

Index Terms: Back-propagation algorithm, defect identification, eco-friendly insulation gas, partial discharge, UHF sensor

I. INTRODUCTION

Gas-insulated switchgear (GIS) is used to improve the reliability of power systems. Sulfur hexafluoride (SF_6) exhibits superior insulation properties, including excellent dielectric strength and arc-quenching performance. Therefore, SF_6 is widely used as an insulator in gas-insulated power equipment. However, its use is severely limited by the Kyoto Protocol and Paris Agreement because of its global warming potential (GWP), which is 23,900 times higher than that of carbon dioxide (CO_2) [1-4]. Therefore, several studies have been conducted to develop eco-friendly alternative gases. Green gas for grid (g^3) has been employed in GIS as one of the most popular substitutes for SF_6, and its insulation breakdown characteristics have been investigated.

g^3 is a gas mixture comprising NOVEC^{TM} 4710, CO_2, and O_2. NOVEC^{TM} 4710 has a good insulation strength, which is approximately twice that of SF_6, an existing insulation gas used in high-voltage gas-insulated switchgear. In addition, it can significantly reduce the GWP [5-8]. Therefore, g^3 is a suitable replacement for SF_6. Several studies have been conducted on the strength of the insulation. The characteristics of the insulation breakdown for g^3 were analyzed using AC and lightning impulse voltages for different electrodes and gas pressures. The results showed that g^3 mixed with 3.7% NOVEC^{TM} 4710 has good dielectric performance for high-voltage insulation, and its insulation strength at 0.67-0.82 MPa is equivalent to 87-96% of that of SF_6 at 0.55 MPa [9-10].

Although the insulation performance of g^3 has been investigated, few studies have been conducted on its partial-discharge (PD) characteristics. PD activity is an indication of the initial insulation deterioration in electrical power equipment prior to insulation breakdown. In addition, identifying

Received 11 June 2023, **Revised** 21 june 2023, **Accepted** 21 June 2023
***Corresponding Author** Sung-Wook Kim (E-mail: number1@silla.ac.kr)
Department of Electrical and Electronics Engineering, Silla University, 46958, Korea

Open Access **https://doi.org/10.56977/jicce.2023.21.3.233** print ISSN: 2234-8255 online ISSN: 2234-8883

PD defects is important for onsite engineers in decision-making for maintenance inside a GIS once PD is detected [11-14]. Various PD characteristics of SF_6 have been investigated to identify the types of PD defects. However, studies on the PD characteristics of g^3 are limited. Therefore, it is necessary to investigate the PD characteristics and identify the types of PD defects in terms of g^3.

This paper describes the identification of PD defects in an eco-friendly insulation gas using a back-propagation algorithm. To simulate PD defects in the GIS, four PD electrode systems, namely, a free-moving particle (FMP), protrusion on conductor (POC), protrusion on enclosure (POE), and voids, were fabricated. An ultrahigh-frequency (UHF) sensor was used to detect the PD signals for onsite continuous PD measurements. The PD parameters were extracted from single PD pulses in the time and frequency domains. Thereafter, phase-resolved partial discharge (PRPD) patterns, and the back-propagation algorithm in the artificial neural network (ANN) was designed to identify the types of PD defects using a virtual instrument (VI) based on LabVIEW.

II. EXPERIMENTAL METHOD

A PD signal is an important indicator of the onset of dielectric breakdown because it is generated by diverse conditions resulting from GIS defects in service. Therefore, detecting PD signals prior to GIS failure is very important. Fig. 1 shows the PD electrode systems of the FMP, POC, POE, and voids used to simulate defects inside the GIS. The FMP is composed of a spherical electrode and an aluminum particle with a diameter of 2 mm on a concave-plane electrode. The POC and POE are composed of a plane electrode of tungsten-copper alloy with a diameter of 80 mm and thickness of 20 mm, and a needle electrode with a curvature radius of 10 µm. The voids consist of two plane electrodes and a void sample.

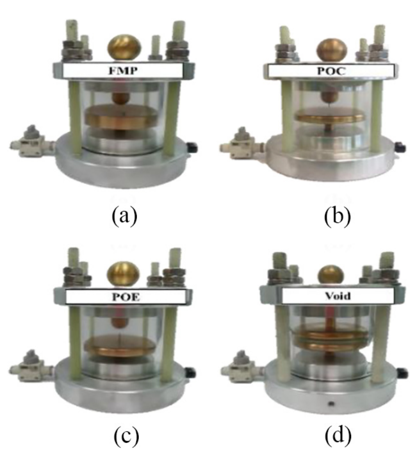

Fig. 1. PD electrode systems.

Fig. 2 shows the experimental configuration used in this study. A transformer with a maximum voltage of 20 kV was used to apply a high voltage to the PD electrode systems. The four PD electrode systems were filled with g^3 at 0.5 MPa. The PD signals were detected using a UHF sensor with a frequency range of 100-2,000 MHz for online PD measurements. In addition, the conventional method according to IEC 60270, which uses a coupling capacitor and a PD measuring device with a frequency range of less than 1 MHz, was used to evaluate the linearity of the UHF sensor for PD signals. The PD signals measured by the UHF sensor were recorded using a digital oscilloscope at a sampling rate of 10 GS/s. A mockup GIS chamber was designed and fabricated to perform PD measurements under actual GIS conditions. A UHF sensor was mounted on the GIS window, and the PD electrode system was placed inside the GIS chamber.

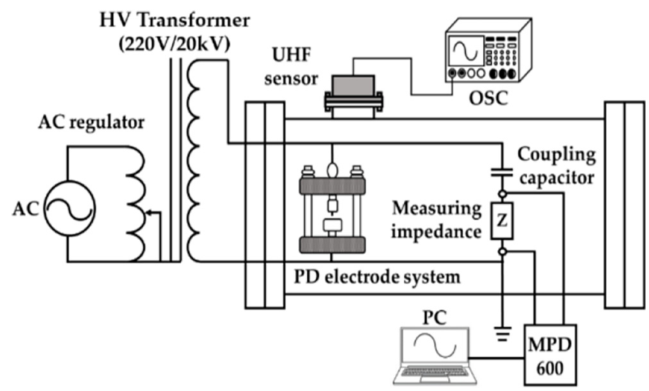

Fig. 2. Experimental configuration.

Prior to the PD experiment, calibration was performed to evaluate the linearity of the UHF sensor. Artificial calibration pulses with an apparent charge of 10-1000 pC were injected into the experimental system. A UHF sensor measured electromagnetic waves generated by calibration pulses with an apparent charge. The calibration results show that

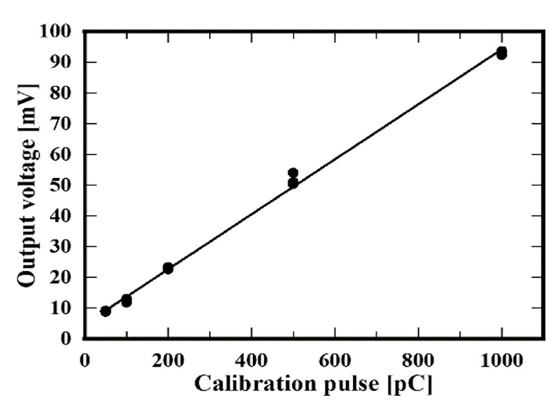

Fig. 3. Calibration result of the UHF sensor.

the output voltage of the UHF sensor is linear in accordance with the calibration pulse, as shown in Fig. 3.

III. RESULTS AND ANALYSIS

To identify the four types of PD defects, a UHF sensor was used to measure typical single pulses in terms of rising time, falling time, and pulse width while maintaining a constant applied voltage. The rising time is the time taken from 10 to 90% of its maximum value, the falling time is the time taken from 90 to 10% of its maximum value, and the pulse width is the time taken to reach 50% of the maximum value. In addition, the frequency spectra of the single pulses were analyzed to determine the maximum frequency. The PRPD patterns were used to analyze the PD characteristics, such as the magnitude, count, and phase of the PD pulses. To confirm the phase of the pulse occurrence, 12 pulse distribution ratios were determined at 30° intervals, ranging from 0° to 360°.

A. Single Pulse

Fig. 4 shows typical single PD pulses and their frequency spectra in g^3 for the four types of PD defects. A summary of the comparison of parameters, such as rising time, falling time, pulse width, and frequency spectrum, is shown in Tables 1 and 2. The parameters are the average values extracted from ten pulses for each case. The pulses in the void exhibited a relatively longer rising time, falling time, and pulse width than those in the others. In terms of the frequency spectrum, the maximum frequency in FMP was higher than those of the others, and there were no differences between POC and POE.

B. PRPD Pattern

The PRPD patterns in g^3 for the different PD defects at the same applied voltage are shown in Fig. 5. In the FMP, the average discharge magnitude and pulse count were 459 mV and 183 N/s. Discharge pulses were observed at phase angles ranging from 0-360°. In POC and POE, the average discharge magnitude and pulse count were 32 mV and 42 N/s and 42 mV and 504 N/s, respectively. Discharge pulses occurred in the POC at phase angles of 61-102°, whereas discharge pulses were observed in the POE at phase angles of 46-130° and 254-302°. In the void, the average discharge magnitude and pulse count were 244 mV and 187 N/s, and the discharge pulses were distributed at phase angles of 16-118° and 182-254°.

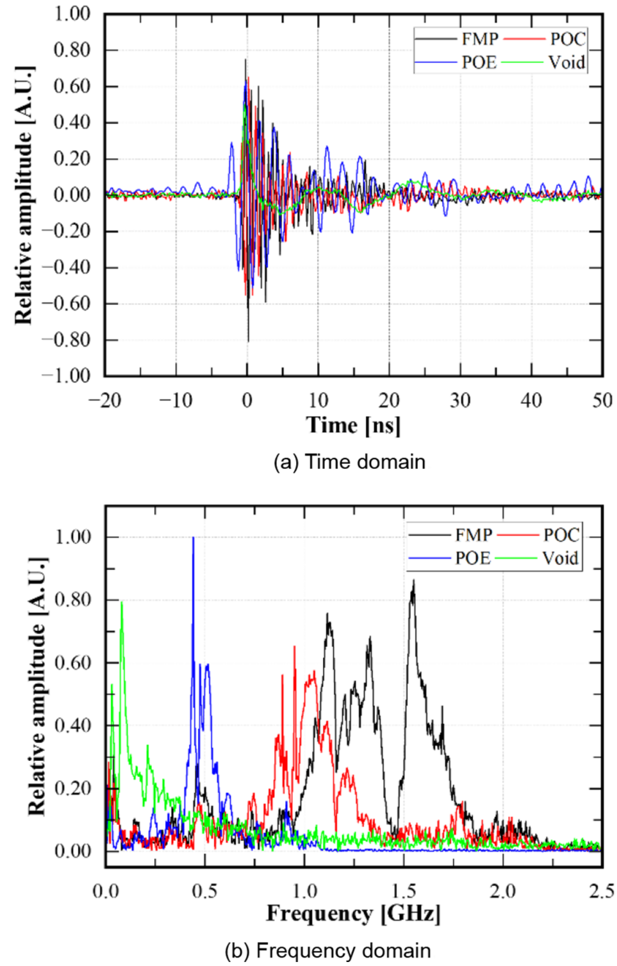

Fig. 4. PD pulse and its frequency spectrum.

Table 1. Comparison of pulse parameters

PD defects	Rising time [ns]	Falling time [ns]	Pulse width [ns]
FMP	0.19	0.17	0.18
POC	0.25	0.22	0.20
POE	0.30	0.25	0.33
Void	0.68	0.90	0.74

Table 2. Comparison of frequency spectra

PD defects	Main frequency ranges [GHz]	Maximum Frequencies (GHz)
FMP	1.0-1.7	1.55
POC	0.8-1.2	0.95
POE	0.8-1.2	0.88
Void	0.1-0.3	0.16

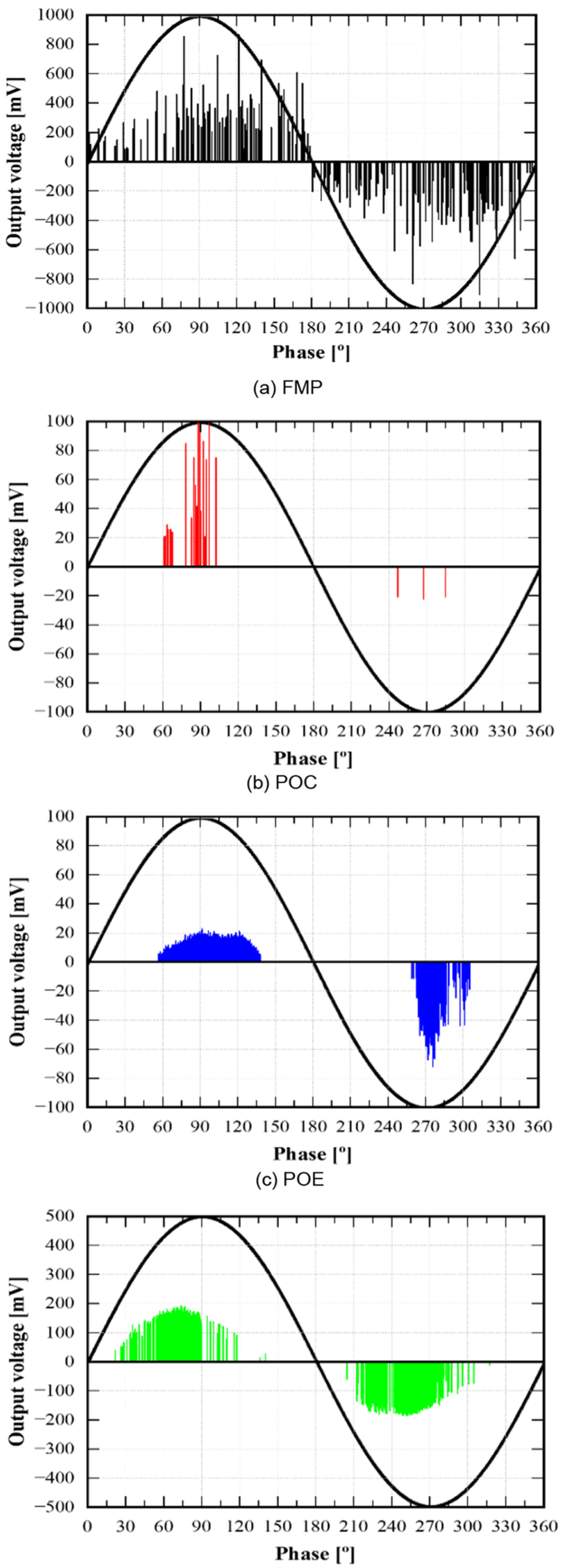

(a) FMP

(b) POC

(c) POE

(d) Void

Fig. 5. PRPD patterns.

C. PD Identification

A back-propagation algorithm with a multilayer structure was designed for PD diagnosis. To identify the four types of PD defects, 18 parameters were extracted in this study, including rising time, falling time, pulse width, maximum frequency, output voltage pulse count, and 12 pulse distribution ratios at 30º intervals in the entire phase of 0 to 360º. As shown in Fig. 6, the backpropagation algorithm consisted of three layers: 18 input, 20 hidden, and four output layers. The input layers receive and transmit the data to the hidden layers. The hidden layer is positioned between the input and output layers and is responsible for the mathematical operations, each designed to produce an output specific to the intended results. During data processing, the hidden layer applies nonlinear transformations for feature extraction from the input layer. The output layer provides a linear combination of the output weights and contains the output of the problem [15]. The extracted PD parameters are trained 20 times according to the type of PD defect in the input layer. Depending on the learning results, the output value was compared with a target value of 1. The differences between the output and target values were calculated, and the back-propagation algorithm was run continuously until the output value approached the target value [16,17]. In this study, the back-propagation algorithm was fabricated using a virtual instrument based on LabVIEW, as shown in Fig. 7.

Eighteen parameters according to four types of PD defects were trained 20 times in the back-propagation algorithm, and

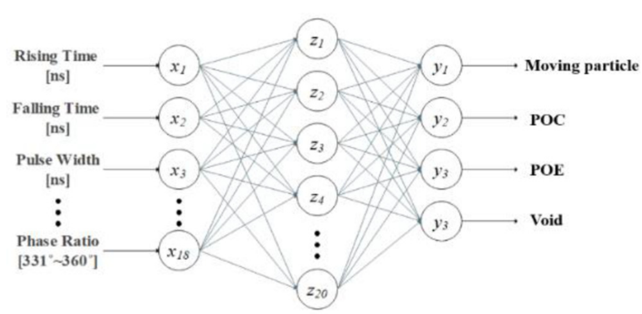

Fig. 6. Structure of the back-propagation algorithm.

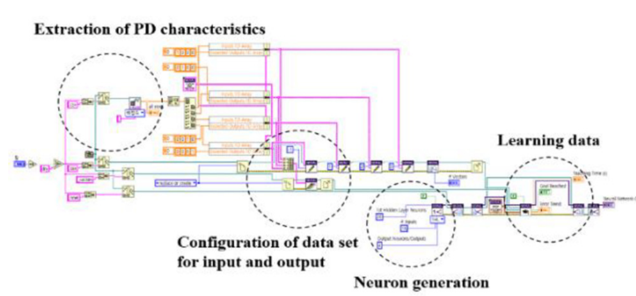

Fig. 7. Example of the back-propagation algorithm.

the learning rate was 0.01 for 977 epochs to obtain an error mean square of 0.001. Thereafter, 50 PD data points were used to evaluate the accuracy. The results show that the back-propagation algorithm proposed in this paper has an accuracy rate of over 90% for identifying the four types of PD defects, as shown in Table 3.

Table 3. Accuracy of identification of PD defects

PD defects	Identification [%]			
	FMP	POC	POE	Void
FMP	98.4	0	0	1.6
POC	0	96.6	2.7	0.7
POE	0	3.4	95.9	0.7
Void	1.2	3.6	3.6	91.6

IV. DISCUSSION AND CONCLUSIONS

This paper describes a method for identifying PD defects in an eco-friendly insulation gas using a back-propagation algorithm. To identify the types of PD defects, a single PD pulse in the time and frequency domains and the PRPD patterns, including the discharge magnitude, pulse count, and phase angle, were determined. In addition, a back-propagation algorithm was designed using virtual instruments based on LabVIEW. Eighteen parameters were extracted from the PD defects and used to train the back-propagation algorithm. Fifty data points corresponding to the four types of PD defects were used to evaluate the accuracy of the back-propagation algorithm in this study. The results confirmed that PD identification had an accuracy rate of over 90%. The experimental results of this study are expected to provide a valuable database for UHF monitoring systems in eco-friendly GIS. In the future, the PRPD characteristics of additional PD defects, such as cracks, particles on spacers, and floating, should be investigated.

ACKNOWLEDGEMENTS

This research was supported by the Basic Science Research Program through the National Research Foundation of Korea (NRF), funded by the Ministry of Education (grant number: 2022R1G1A1011043).

REFERENCES

[1] S. W. Kim, J. R. Jung, Y. M. Kim, G. S. Kil, and G. Wang, "New diagnosis method of unknown phase-shifted PD signals for gas insulated switchgears," *IEEE Transaction on Dielectrics and Electrical Insulation*, vol. 25, no. 1, pp. 102-109, Feb. 2018. DOI: 10.1109/TDEI.2018.006739.

[2] G. M. Wang and G. S. Kil, "Measurement and analysis of partial discharge using an ultra-high frequency sensor for gas insulated structures," *Metrology and Measurement Systems*, vol. 24, no. 3, pp. 515-524, Sep. 2017. DOI: 10.1515/mms-2017-0045.

[3] A. Beroual and A. Haddad, "Recent advances in the quest for a new insulation gas with a low impact on the environment to replace sulfur hexafluoride (SF6) gas in high-voltage power network applications," *Energies*, vol. 10, no. 8, p. 1216, Aug. 2017. DOI: 10.3390/en10081216.

[4] Intergovernmental Panel on Climate Change. *Cambridge University Press: New York*, NY, USA, pp. 159-254, 2013.

[5] F. Ye, X. Zhang, Y. Li, Y. Li, Z. Wei, S. Xiao, and S. Tian, "AC breakdown strength and its by-products of eco-friendly perfluoroisobutyronitrile/O_2/N_2 Gas Mixture at High Pressure for HV Equipment," *IEEE Transaction on Dielectrics and Electrical Insulation*, vol. 28, no. 3, pp. 1020-1027, Jun. 2021. DOI: 10.1109/TDEI.2021.009463.

[6] B. Zhang, N. Uzelac, and Y Cao, "Fluoronitrile/CO_2 mixture as an eco-friendly alternative to SF6 for medium voltage switchgears," *IEEE Transaction on Dielectrics and Electrical Insulation*, vol. 25, no. 4, pp. 1340-1350, Aug. 2018. DOI: 10.1109/TDEI.2018.007146.

[7] G. Wang, W. H. Kim, G. S. Kil, S. W. Kim, and J. R. Jung, "Green gas for a grid as an eco-friendly alternative insulation gas to SF6: from the perspective of partial discharge under AC," *Applied Sciences*, vol. 9, no. 4, p. 651, Feb. 2019. DOI: 10.3390/app9040651.

[8] H. E. Nechmi, A. Beroual, A. Girodet, and P. Vinson, "Effective ionization coefficients and limiting field strength of fluoronitriles-CO_2 mixtures," *IEEE Transaction on Dielectrics and Electrical Insulation*, vol. 24, no. 2, pp. 886-892, Apr. 2017. DOI: 10.1109/TDEI.2017.006538.

[9] Y. Kieffel, T. Irwin, P. Ponchon, and J. Owens, "Green gas to replace SF6 in Electrical Grids," *IEEE Power and Energy Magazine*, vol. 14, no. 2, pp. 32-39, Mar. 2016. DOI: 10.1109/MPE.2016.2542645.

[10] H. E. Nechmi, A. Beroual, A. Girodet, and P. Vinson, "Fluoronitriles/CO_2 gas mixture as promising substitute to SF6 for insulation in high voltage applications," *IEEE Transactions on Dielectrics and Electrical Insulation*, vol. 23, no. 5, pp. 2587-2593, Oct. 2016. DOI: 10.1109/TDEI.2016.7736816.

[11] A. Beroual and A. Haddad, "Recent advances in the quest for a new insulation gas with a low impact on the environment to replace sulfur hexafluoride (SF6) gas in high-voltage power network applications," *Energies*, vol. 10, no. 8, p. 1216, Aug. 2017. DOI: 10.3390/en10081216.

[12] CIGRE Working Group D1.33. Guide for Partial Discharge Measurements in Compliance to IEC 60270; Technical Brochure No. 366, CIGRE Paris, France, 2008.

[13] H. D. Ilkhechi and M. H. Samimi, "Application of the acoustic method in partial discharge measurement: A review," *IEEE Transaction on Dielectrics and Electrical Insulation*, vol. 28, no. 1, pp. 42-51, Feb. 2021. DOI: 10.1109/TDEI.2020.008985.

[14] A. Lapp and H. G. Kranz, "The use of the CIGRE data format for PD diagnosis applications," *IEEE Transaction on Dielectrics and Electrical Insulation*, vol. 7, no. 1, pp. 102-112, Feb. 2000. DOI: 10.1109/94.839347.

[15] W. Y. Chang, "Partial discharge pattern recognition of cast resin current transformers using radial basis function neural network," *Journal of Electrical Engineering and Technology*, vol. 9, no. 1, pp. 293-300, Jan. 2014. DOI: 10.5370/JEET.2014.9.1.293.

[16] M. N. Danikas, N. Gao, and M. Aro, "Partial discharge recognition using neural network: A review," *Electrical Engineering*, vol. 85, pp. 87-95, May 2003. DOI: 10.1007/s00202-002-0151-5.

[17] N. Hozumi, T. Okamoto, and T. Imajo, "Discrimination of partial discharge patterns using neural network," *IEEE Transaction on Dielectrics and Electrical Insulation*, vol. 27, no. 3, pp. 550-556, Jun. 1992. DOI: 10.1109/14.142718.

Sung-Wook Kim
received the BEng, MEng, and PhD degrees in electrical engineering and high voltage engineering from the Korea Maritime University, Korea in 2008, 2010 and 2017, respectively. He worked for R&D center of Hyosung Corporation and was one of the members in charge of DGA and PD project for 9 years. He is currently a professor at Silla University, Korea. His research interests are PD and DGA measurements of high-voltage transformers and gas insulated switchgear. Now he is currently performing two projects related to PD diagnosis of eco-friendly GIS and cast-resin power transformer.